Two-level masers as heat-to-work converters

Arnab Ghosh[a,b], David Gelbwaser-Klimovsky[c], Wolfgang Niedenzu[b,d], Alexander I. Lvovsky[e,f,g,h], Igor Mazets[i,j], Marlan O. Scully[k,l,m,1], and Gershon Kurizki[b]

[a]Department of Physics, Shanghai University, Shanghai 200444, People's Republic of China; [b]Department of Chemical and Biological Physics, Weizmann Institute of Science, Rehovot 7610001, Israel; [c]Department of Chemistry and Chemical Biology, Harvard University, Cambridge, MA 02138; [d]Institut für Theoretische Physik, Universität Innsbruck, A-6020 Innsbruck, Austria; [e]Institute for Quantum Science and Technology, University of Calgary, Calgary, AB T2N 1N4, Canada; [f]International Center for Quantum Optics and Quantum Technologies (Russian Quantum Center), Skolkovo, Moscow 143025, Russia; [g]Institute of Fundamental and Frontier Sciences, University of Electronic Science and Technology, Chengdu, Sichuan 610054, China; [h]Clarendon Laboratory, University of Oxford, Parks Road, Oxford OX1 3PU, United Kingdom; [i]Atominstitut, Technische Universität Wien, 1020 Vienna, Austria; [j]Wolfgang Pauli Institute, Universität Wien, 1090 Vienna, Austria; [k]Institute for Quantum Science and Engineering, Texas A&M University, College Station, TX 77843; [l]Department of Mechanical and Aerospace Engineering, Princeton University, Princeton, NJ 08544; and [m]Department of Physics, Baylor University, Waco, TX, 76798

Contributed by Marlan O. Scully, August 13, 2018 (sent for review April 2, 2018; reviewed by Jianshu Cao and H. Eugene Stanley)

Heat engines, which cyclically transform heat into work, are ubiquitous in technology. Lasers and masers may be viewed as heat engines that rely on population inversion or coherence in the active medium. Here we put forward an unconventional paradigm of a remarkably simple and robust electromagnetic heat-powered engine that bears basic differences to any known maser or laser: The proposed device makes use of only one Raman transition and does not rely on population inversion or coherence in its two-level working medium. Nor does it require any coherent driving. The engine can be powered by the ambient temperature difference between the sky and the ground surface. Its autonomous character and "free" power source make this engine conceptually and technologically enticing.

maser | heat | laser

A maser or a laser is typically based on a medium with three or more levels wherein one transition is pumped to establish population inversion on another (signal) transition (1). Alternatively, pumping may serve to induce coherence between a set of levels, as in the case of lasers without inversion (LWI) (2). Either scheme results in the pump conversion into a coherent, amplified signal output.

A much less emphasized aspect of lasers and masers is their analogy to heat engines. This analogy was pointed out by Scovil and Schulz-DuBois (SSD) (3) who related the maximal conversion efficiency of a three-level maser to the Carnot efficiency bound (4) by assuming that one transition is pumped by a hot bath and another is coupled to a cold bath. The three-level SSD scheme (*SI Appendix*, Fig. S1) has become a canonical microscopic model for heat engines (5, 6) and their quantum-mechanical characteristics (7–9).

In view of the extensive developments in the area of quantum heat engines (10–21), we find it timely to revisit the rapport between masers and heat engines. To this end, we put forward an unconventional operational paradigm of a remarkably simple, heat-powered maser. Against the common view that at least two transitions are needed for a maser/laser, the proposed device uses only one (two-photon, i.e., Raman) transition and its working medium (WM) is well approximated by uninverted two-level systems (TLSs). We identify the work (22–24) output of the proposed device with the useful (noiseless) portion of the amplified signal. We find that neither the input nor the output need be fully coherent to come close to the highest (SSD) efficiency.

The basic ingredients of the envisaged device are (Fig. 1*A*) (*i*) hot and cold heat baths, realized by ambient thermal radiation that is filtered into spectrally distinct modes of (infrared or microwave) narrow-band cavities; (*ii*) a WM consisting of TLSs that are continuously (6, 14) [rather than intermittently, as in Otto or Carnot cycles (10, 17, 20)] coupled to the hot and cold baths (cavity modes); and (*iii*) a microwave or infrared-signal mode which acts as a "piston" that extracts the work.

The two levels of the WM are coupled to the cold bath near a frequency ω_0 and (via a two-photon transition) to the hot bath near the frequency ω_h as well as to the signal near $\nu = \omega_h - \omega_0$. The heat-to-work conversion consists of photon absorption from the hot bath, reemission into the cold bath, and production of a signal photon at the difference frequency.

Because the WM interacts with the cold bath resonantly and hence more strongly than with the hot bath, the WM can be assumed to be close to the temperature of the former. Then the imbalance between the populations of the hot bath and the WM can lead to amplification of the signal mode.

Operational Principle

We consider the WM whose $|e\rangle \leftrightarrow |g\rangle$ transition at frequency ω_0 is near resonant with a cold bath (c) and is in a two-photon (Raman) resonance with the signal mode at frequency ν and the hot-bath (h) modes near frequency ω_h (Fig. 1*B*). The effective Hamiltonians of the interaction between the WM and the two baths in the interaction picture and the rotating-wave approximation (RWA) are $V_c(t)$ and $V_h(t)$, respectively. They are written in terms of $a_k^{(c,h)}$ and $\mathrm{b}^\dagger$, the mode annihilation and creation operators of the two baths and signal, respectively. While the Hamiltonian $V_c(t)$ for resonant system–bath coupling composed of $|e\rangle\langle g|\, a_k^{(c)}$ terms is well known (2), the unconventional Raman-coupling Hamiltonian $V_h(t)$ consisting of $|e\rangle\langle g|\, \mathrm{b}^\dagger a_k^{(h)}$ is derived in *SI Appendix, Derivation of the Raman Hamiltonian*.

Because, as mentioned above, the WM interacts mainly with the near-resonant cold bath at temperature T_c (i.e., $V_h(t)$ has much weaker effect than $V_c(t)$), it attains a steady state whose

Significance

We propose a paradigm of heat-powered maser. In contrast to textbook knowledge, it does not require population inversion or coherent driving and hence can operate with a two-level working medium. Therefore, it is a conceptually different type of maser and, more generally, a conceptually different quantum heat machine. Its autonomous character and "free" power source make this machine technologically enticing.

Author contributions: A.G., G.K., and M.O.S. designed research; A.G., D.G.-K., W.N., A.I.L., I.M., M.O.S., and G.K. performed research; and A.G., G.K., A.I.L., and M.O.S. wrote the paper.

Reviewers: J.C., Massachusetts Institute of Technology; and H.E.S., Boston University.

The authors declare no conflict of interest.

[1]To whom correspondence should be addressed. Email: scully@tamu.edu.

This article contains supporting information online at www.pnas.org/lookup/suppl/doi:10.1073/pnas.1805354115/-/DCSupplemental.

Published online September 18, 2018.

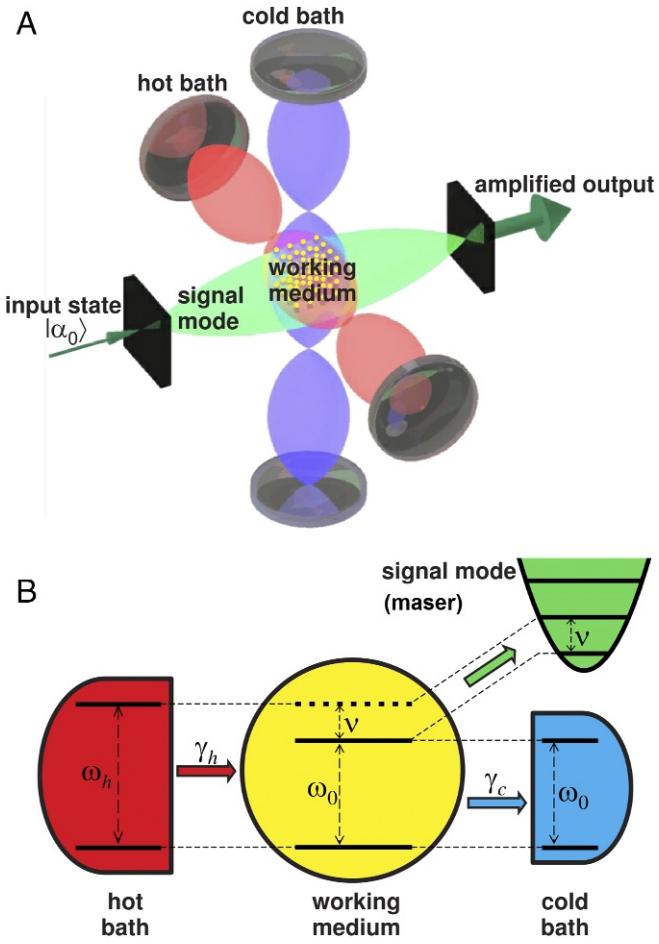

Fig. 1. (*A*) The proposed quantum heat engine acting as a maser. The two narrow-band cavities spectrally filter the hot and cold baths. The working medium consists of TLSs with energy-level distance ω_0 and an off-resonant microwave or infrared signal (green) at frequency ν. The two black mirrors define the signal mode but they are not essential for maser operation in the single-pass amplifier regime of the signal. (*B*) A thermodynamic outline of the proposed scheme.

upper- and lower-level populations ρ_{ee} and ρ_{gg} are related by

$$\frac{\rho_{ee}}{\rho_{gg}} \simeq \exp\left(-\frac{\hbar\omega_0}{k_{\rm B}\,T_c}\right) = \frac{\bar{n}_c}{\bar{n}_c+1}, \qquad [1]$$

where

$$\bar{n}_{c,h} = \left[\exp\left(\frac{\hbar\omega_{0,h}}{k_{\rm B}\,T_{c,h}}\right) - 1\right]^{-1} \qquad [2]$$

are the photon occupancies of the two baths. The knowledge of this steady state now allows us to find the evolution of the signal field as a mediator of the interaction between the WM and the hot bath. From the master equation for the signal mode, taking the limit where the signal mode is treated semiclassically (*SI Appendix, Evolution of the signal state*), one can obtain a rate equation for the signal-mode intensity (mean energy) in the single-pass amplifier regime (2)

$$\begin{aligned} \dot{I}_s &= G I_s \\ G &= 2\gamma_h\,[\rho_{gg}\bar{n}_h - \rho_{ee}(\bar{n}_h+1)], \end{aligned} \qquad [3]$$

where G, the gain of our maser, is proportional to γ_h, the transition rate associated with the Raman coupling constant, and the factor in the square brackets that expresses the difference between the photon stimulated-emission probability $\rho_{gg}\bar{n}_h$ and its absorption $\rho_{ee}(\bar{n}_h+1)$ induced by the hot bath. This nonstandard factor allows for gain from an uninverted WM, as shown below.

The gain (3) can be rewritten with the help of Eq. **1** as

$$G = \gamma_h \frac{2(\bar{n}_h - \bar{n}_c)}{2\bar{n}_c + 1}. \qquad [4]$$

This means that $G \geq 0$, above or at the amplification threshold, corresponds to $\bar{n}_h(\omega_h) \geq \bar{n}_c(\omega_0)$ and hence to

$$\frac{\omega_h}{T_h} \leq \frac{\omega_c}{T_c}. \qquad [5]$$

The energy $\hbar\omega_h$ of a hot-bath photon is shared between the signal-mode and cold-bath photons, with energies $\hbar\nu$ and $\hbar\omega_c$, respectively. This sets the limit on the efficiency of our engine, defined as the ratio of the extracted energy in the signal mode to the heat input from the hot bath.

Since $\omega_c = \omega_h - \nu$, this efficiency (conforming to Eqs. **3**–**5**) satisfies

$$\eta = \eta_{\rm SSD} = \frac{\nu}{\omega_h} \leq 1 - \frac{T_c}{T_h}, \qquad [6]$$

where the equality holds at threshold in the semiclassical regime for the signal. Namely, we recover the SSD relation (3) for the engine efficiency at the threshold point whereby the signal to the hot-pump frequency ratio corresponds to the Carnot limit. Below threshold, i.e., for $G < 0$, the device acts as a refrigerator: It consumes the signal power to move heat from the cold to the hot bath (5).

In contrast to the SSD model for a maser, here the WM is uninverted and no other transition is practically involved (although the Raman process presumes a far-detuned, additional empty level). Thermal-occupancy imbalance of the two baths $\bar{n}_h(\omega_h) > \bar{n}_c(\omega_0)$ at two different frequencies, ω_h and ω_0, rather than population inversion of the levels, $\rho_{ee} > \rho_{gg}$ in a conventional (SSD) maser, is the requirement for the output signal intensity to exceed its input counterpart in a single pass.

The present model, which uses Raman coupling to the virtual level, still shares common thermodynamic properties with the three-level SSD maser, in particular, the Carnot bound for the efficiency. However, the Carnot bound is practically useless since it is attained in the regime of vanishing power output. Interestingly, a recent study (25) investigates the efficiency at the maximum power (EMP) of the SSD model and demonstrates that the same EMP bound holds for its four-level counterpart. Given the similarity between the SSD model and the proposed model, it may be worthwhile to investigate whether similar bounds are also obtained for the two-level counterpart.

Quantized Photonic Work

The above discussion has assumed, as is common for heat machines (4, 6, 14), that the piston (here the signal mode) is semiclassical and its entropy is negligible (hence it is often referred to as a work reservoir). However, in the case of a microscopic input signal, we must allow for the "heating up" of the signal mode (7). That is, part of the energy acquired by the piston leads to its entropy increase and cannot be extracted as useful work.

To find the maximal work (22–24) extractable from the signal mode, a fully quantum treatment of this mode is required. To this end we consider the evolution of the Glauber–Sudarshan P function of the signal mode (2, 26, 27), governed by a Fokker–Planck equation (*SI Appendix, Evolution of the signal state*). For an initial coherent state $|\alpha_0\rangle$ we find that the distribution (in the interaction picture) evolves as

$$P(\alpha, t) = \frac{1}{\pi\sigma^2(t)} \exp\left[-\frac{|\alpha - \alpha_0 e^{Gt/2}|^2}{\sigma^2(t)}\right]. \qquad [7]$$

Thus, the distribution is shifted outward by $\alpha_0 e^{Gt/2}$ and its width grows (during the single-pass transit time t) as

$$\sigma^2(t) = \frac{\bar{n}_h(\bar{n}_c+1)}{\bar{n}_h-\bar{n}_c}(e^{Gt}-1). \quad [8]$$

That is, a coherent state at the input becomes a displaced thermal state at the output (Fig. 2*A*). The mean energy of this state is (28)

$$\langle H_s(t)\rangle = \hbar\nu\left[|\alpha_0|^2 e^{Gt}+\sigma^2(t)\right], \quad [9]$$

where the first term in the brackets corresponds to the coherent amplitude and the second one to the thermal contribution.

For a given signal state ρ_s, the ergotropy (19, 22–24, 29), which is the maximal extractable work from that state, is expressed by

$$\mathcal{W}(\rho_s) = \langle H(\rho_s)\rangle - \langle H(\rho_s^{\rm pas})\rangle. \quad [10]$$

Here $\rho_s^{\rm pas}$ is a passive state: It is defined as the state with the least energy that is accessible from ρ_s via a unitary transformation. Namely, Eq. **10** expresses the maximal energy change that can be effected unitarily, without entropy change, which is the definition of work (19) extractable from the signal.

In the displaced-thermal state output, the $\hbar\nu\sigma^2(t)$ term in expression **9** for the energy corresponds to a passive state. Indeed, the phase-space displacement operator $\mathcal{D}(-\alpha) = e^{-\alpha a^\dagger + \alpha^* a}$ for $\alpha = \alpha_0 e^{Gt/2}$ applied to the amplified signal mode at t will transform it to a thermal state centered at the phase-space origin. This operation is unitary and hence isentropic. The resulting thermal state of energy $\hbar\nu\sigma^2(t)$, on the other hand, is entirely passive (30) and permits no further work extraction. Hence the ergotropy of the output state is $\mathcal{W}(t) = \hbar\nu|\alpha_0|^2 e^{Gt}$.

The displacement operator that extracts the work can be realized by overlapping the target state on a highly reflective beam splitter (31, 32) with a strong coherent local oscillator field (Fig. 2*B* and *SI Appendix, Implementation of the displacement operator*).

The efficiency of the engine with a coherent state $|\alpha_0\rangle$ at the input is found to be always less than that of its classical counterpart, but approaches it for high input-state amplitude (Fig. 2 *C* and *D*). If the engine is operated by injecting independent coherent states with arbitrary mean phases, whose amplitudes are distributed according to $p(|\alpha_0|)$, the upper bound on the mean efficiency can be calculated to be (*SI Appendix, Derivation of the maser efficiency*)

$$\langle\eta\rangle = \frac{\nu}{\omega_h}\int \frac{|\alpha_0|^2}{|\alpha_0|^2+\frac{\bar{n}_h(\bar{n}_c+1)}{\bar{n}_h-\bar{n}_c}}|\alpha_0|p(|\alpha_0|)\mathrm{d}|\alpha_0| \leqslant \eta_{\rm SSD}. \quad [11]$$

We see that efficiencies up to the SSD limit are obtainable provided the mean initial amplitude $\langle|\alpha_0|\rangle$ is well above 1 and dominates over the thermal term $\bar{n}_h(\bar{n}_c+1)/(\bar{n}_h-\bar{n}_c)$.

The upper bound on the efficiency in Eq. **11**, which is given by the equality sign, requires a local oscillator in Fig. 2*B* that is adapted to the amplitude and phase of each initial coherent state. Namely, phase and amplitude estimation on the input would be beneficial to properly adjust the local oscillator phase. However, phase variance of the signal below 1 suffices, so that it can properly interfere with the local oscillator.

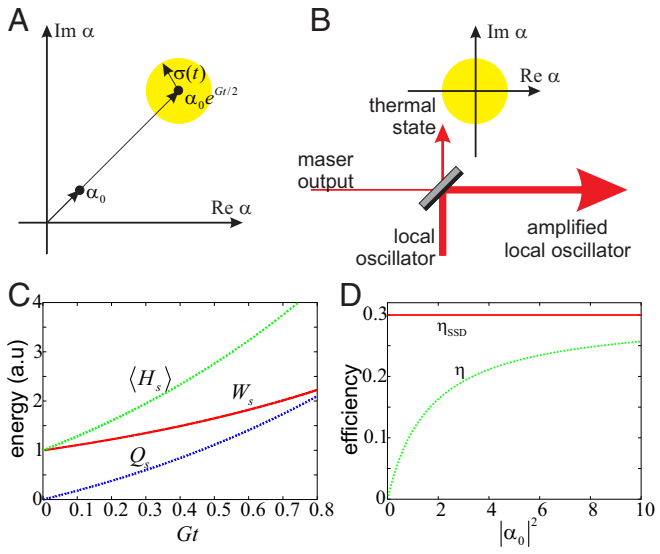

Fig. 2. Amplification of the signal state. (*A*) The Glauber–Sudarshan *P* function of an initial coherent state $|\alpha_0\rangle$ and the amplified state. The initial *P* function is singular while the final state is a displaced thermal state which has a finite width $\sigma(t)$. (*B*) Separation of the active (work-producing) and passive (heat-producing) components of the signal output by the displacement operator implemented via a beam splitter (BS) transformation. (*C*) Amplification of a small (few-photon) signal, well below the saturation regime: The passive (thermal) energy Q_s, ergotropy (or work) $\mathcal{W}_s$, and total mean energy $\langle H_s\rangle$ are plotted for initial $|\alpha_0|^2 = 1$ as a function of the gain (*G*) (Eq. **4**), multiplied by the transit time *t*. (*D*) Efficiency η [work output divided by the heat input (*SI Appendix, Derivation of the maser efficiency*, Eq. **S31**)] as a function of the mean-squared amplitude $|\alpha_0|^2$ tends to the semiclassical efficiency $\eta_{\rm SSD} = \nu/\omega_h$ limited by the Carnot bound for large initial-state amplitudes $|\alpha_0|$. The parameters for *C* and *D* are $\nu/\omega_h = 0.3$, $\gamma_h/\nu = 0.033$, and $T_h = 2.33T_c$.

Proposed Experimental Setups

The envisioned experiments may be conducted with thermal atoms or molecules in microwave cavities (2). One cavity mode can be in contact with either solar radiation or air and the other one with the colder ground (earth surface). The corresponding hot and cold bath-temperature differences may range from hundreds to tens of kelvins (Fig. 1). The WM may consist of, e.g., molecules in a host lattice at room temperature, with a dipolar transition $\omega_0 > 1.45$ GHz. Whereas optical pumping is normally required for their population inversion (33, 34), it is not needed in the proposed scheme: In the engine considered above, ambient heat may be converted to work at the signal frequency $\nu \gtrsim 1$ MHz: for Raman coupling $g_k \gtrsim 5-10$ Hz and a solid matrix of atoms or molecules with densities $\sim 10^{18}$ cm^{-3}, we may obtain a gain rate $G \gtrsim 100$ kHz.

In our quest for an optimized WM, we may consider a transition with a giant transition dipole between two Rydberg levels with ω_0 in the gigahertz range. Similar gain rates as in the example above may then be obtained with much lower Rydberg-atom densities of $\sim 10^{12}$ cm^{-3}. The downside of this implementation is that it requires pumping of the lower level in the Rydberg transition. The upside is that the power output from a Rydberg atom ^{87}Rb in the level $n = 68$ may be higher by three orders of magnitude (per atom) than in ref. 17 [where the power per particle (ion) is 3.4×10^{-24} W].

Conclusions

The analysis of the proposed schemes indicates the experimental feasibility of a hitherto unexplored principle: a two-level maser powered by heat and its ability to act as a photonic heat engine. The scheme is universal: We can always choose a transition at frequency ω_0 to be resonant with the cold-bath cavity mode and tune the signal to the frequency difference ν between the hot and cold cavity modes, so that the signal is amplified at the expense

PHYSICS

of the difference between thermal-quanta occupancies of the two cavity modes.

We have seen that for maximal work extraction the required property of the signal-mode output is to be as different as possible from a passive state. The phase spread of the input may be much larger than that of the relevant coherent state. As long as the input mean phase variance is below 1 during repeated operations of the engine, work extraction is straightforward by mixing the output signal with a local oscillator.

From the technological point of view the ability to extract useful photonic work (power) by an autonomous engine from ambient heat at the temperature difference between, say, the atmosphere and the ground surface is highly advantageous. Strikingly, the proposed maser, in which the heat exchange between the hot and cold baths mediated by the two-level working medium amplifies the signal field, can attain high efficiency even if the signal field is not fully coherent.

ACKNOWLEDGMENTS. We acknowledge the support of the US–Israel Binational Science Foundation (G.K. and M.O.S.), Air Force Office of Scientific Research Award FA9550-18-1-0141, Office of Naval Research Award N00014-16-1-3054, Robert A. Welch Foundation Grant A-1261 (to M.O.S.), the Israeli Science Foundation and Deutsche Forschungsgemeinschaft (G.K.), Natural Sciences and Engineering Research Council (A.I.L.), and Austrian Science Foundation Project P 25329-N27) (to I.M.). A.I.L. is a Canadian Institute for Advanced Research Fellow. W.N. acknowledges support from an Erwin Schrödinger Center for Quantum Science & Technology fellowship of the Austrian Academy of Sciences.

1. Bertolotti M (1983) *Masers and Lasers: An Historical Approach* (CRC Press, New York).
2. Scully MO, Zubairy MS (1997) *Quantum Optics* (Cambridge Univ Press, Cambridge, UK).
3. Scovil HED, Schulz-DuBois EO (1959) Three-level masers as heat engines. *Phys Rev Lett* 2:262–263.
4. Callen HB (1985) *Thermodynamics and an Introduction to Thermostatistics* (Wiley, Singapore).
5. Boukobza E, Tannor DJ (2007) Three-level systems as amplifiers and attenuators: A thermodynamic analysis. *Phys Rev Lett* 98:240601.
6. Kosloff R, Levy A (2014) Quantum heat engines and refrigerators: Continuous devices. *Annu Rev Phys Chem* 65:365–393.
7. Gelbwaser-Klimovsky D, Alicki R, Kurizki G (2013) Work and energy gain of heat-pumped quantized amplifiers. *Europhys Lett* 103:60005.
8. Scully MO, Chapin KR, Dorfman KE, Kim MB, Svidzinsky A (2011) Quantum heat engine power can be increased by noise-induced coherence. *Proc Natl Acad Sci USA* 108:15097–15100.
9. Uzdin R, Levy A, Kosloff R (2015) Equivalence of quantum heat machines, and quantum-thermodynamic signatures. *Phys Rev X* 5:031044.
10. Scully MO, Zubairy MS, Agarwal GS, Walther H (2003) Extracting work from a single heat bath via vanishing quantum coherence. *Science* 299:862–864.
11. Rio Ld, Åberg J, Renner R, Dahlsten O, Vedral V (2011) The thermodynamic meaning of negative entropy. *Nature* 474:61–63.
12. Skrzypczyk P, Short AJ, Popescu S (2014) Work extraction and thermodynamics for individual quantum systems. *Nat Commun* 5:4185.
13. Pekola JP (2015) Towards quantum thermodynamics in electronic circuits. *Nat Phys* 11:118–123.
14. Gelbwaser-Klimovsky D, Niedenzu W, Kurizki G (2015) Thermodynamics of quantum systems under dynamical control. *Adv Mol Opt Phys* 64:329–407.
15. Lostaglio M, Jennings D, Rudolph T (2015) Description of quantum coherence in thermodynamic processes requires constraints beyond free energy. *Nat Commun* 6:6383.
16. Brandão F, Horodecki M, Ng N, Oppenheim J, Wehner S (2015) The second laws of quantum thermodynamics. *Proc Natl Acad Sci USA* 112:3275–3279.
17. Roßnagel J, et al. (2016) A single-atom heat engine. *Science* 352:325–329.
18. Vinjanampathy S, Anders J (2016) Quantum thermodynamics. *Contemp Phys* 57: 545–579.
19. Niedenzu W, Mukherjee V, Ghosh A, Kofman AG, Kurizki G (2018) Quantum engine efficiency bound beyond the second law of thermodynamics. *Nat Commun* 9:165.
20. Kosloff R, Rezek Y (2017) The quantum harmonic Otto cycle. *Entropy* 19:136.
21. Klatzow J, et al. (2017) Experimental demonstration of quantum effects in the operation of microscopic heat engines. arXiv:1710.08716.
22. Pusz W, Woronowicz SL (1978) Passive states and KMS states for general quantum systems. *Commun Math Phys* 58:273–290.
23. Lenard A (1978) Thermodynamical proof of the Gibbs formula for elementary quantum systems. *J Stat Phys* 19:575–586.
24. Allahverdyan AE, Balian R, Nieuwenhuizen TM (2004) Maximal work extraction from finite quantum systems. *Europhys Lett* 67:565.
25. Dorfman KE, Xu D, Cao J (2018) Efficiency at maximum power of a laser quantum heat engine enhanced by noise-induced coherence. *Phys Rev E* 97:042120.
26. Gardiner CW, Zoller P (2000) *Quantum Noise* (Springer, Berlin).
27. Walls DF, Milburn GJ (1994) *Quantum Optics* (Springer, Berlin), 1st Ed.
28. Leonhardt U (1997) *Measuring the Quantum State of Light*, *Cambridge Studies in Modern Optics* (Cambridge Univ Press, Cambridge, United Kingdom).
29. Ghosh A, Latune CL, Davidovich L, Kurizki G (2017) Catalysis of heat-to-work conversion in quantum machines. *Proc Natl Acad Sci USA* 114:12156–12161.
30. Skrzypczyk P, Silva R, Brunner N (2015) Passivity, complete passivity, and virtual temperatures. *Phys Rev E* 91:052133.
31. Paris MG (1996) Displacement operator by beam splitter. *Phys Lett A* 217:78–80.
32. Lvovsky AI, Babichev SA (2002) Synthesis and tomographic characterization of the displaced Fock state of light. *Phys Rev A* 66:011801.
33. Oxborrow M, Breeze JD, Alford NM (2012) Room-temperature solid-state maser. *Nature* 488:353–356.
34. Singer J (2013) *Masers* (Literary Licensing, LLC, Whitefish, MT).